

1300nm-Range GaInNAs-Based Quantum Well Lasers with High Characteristic Temperature

by Hitoshi Shimizu* , Kouji Kumada* , Seiji Uchiyama* and Akihiko Kasukawa*

ABSTRACT Long wavelength-GaInNAsSb SQW lasers that include a small amount of Sb were successfully grown by gas-source molecular beam epitaxy (GSMBE) on a GaAs substrate for application with peltier-free devices of access networks and vertical cavity surface emitting lasers (VCSELs). The GaInNAsSb lasers oscillated under CW operation at 1.258 μm at room temperature. A low CW threshold current of 12.4 mA and a high characteristic temperature (T_0) of 157 K were obtained for GaInNAsSb lasers, which is the best result for GaInNAs-based narrow stripe lasers. Further, GaInNAsSb laser oscillated under CW conditions of over 100°C. A low CW threshold current of 6.3 mA and a high characteristic temperature (T_0) of 256 K were obtained for GaInAsSb lasers, which is also the best result for 1.2 μm -range highly strained GaInAs-based narrow stripe lasers. As a result, GaInNAsSb lasers are very promising for realizing peltier-free access networks and VCSELs.

1. INTRODUCTION

Long wavelength lasers emitting at 1.2~1.3 μm grown on GaAs substrates have been attracting much interest. GaInNAs¹⁻³⁾, GaInAs quantum film (QF), GaAsSb, and InAs quantum dots (QD) have been reported to realize this wavelength on GaAs substrates. Among the candidates, the large conduction band offset can be realized for GaInNAs and highly strained GaInAs QF, which leads to strong electron confinement in wells and to a high characteristic temperature (T_0). The large T_0 of 127~274 K^{1, 2)}, which are much larger than the conventional long-wavelength GaInAsP/InP system, have been reported with these materials. Therefore, a low-cost peltier-free system for access networks can be realized using GaInNAs or highly strained GaInAs QF lasers. Further, there are advantages for a long-wavelength vertical cavity surface emitting laser (VCSEL) on GaAs substrates that it can be grown monolithically on GaAs/AlGaAs DBR mirror with high reflectivity and high thermal conductivity, and it can utilize the mature technology of 850~980 nm VCSELs such as AlAs selective oxidation.

However, most published results referred to broad area laser characteristics with respect to GaInNAs and highly strained GaInAs QW lasers, and there are few results so far for narrow stripe lasers. The large T_0 (148~204 K) were reported on narrow stripe GaInNAs lasers, but the threshold current (I_{th}) was very high (75~500 mA)^{1, 2)}. Recently, a GaInNAs laser with a low threshold current at

room temperature ($I_{\text{th}} = 11$ mA) was reported³⁾, but this laser has a relatively low T_0 of 70~80 K³⁾.

To obtain 1.3 μm -GaInNAs lasers with good crystalline quality, 1.2 μm -range GaInAs QF lasers that have strong photoluminescence intensity have to be grown, because nitride makes photoluminescence intensity poor.

A few 1.2 μm -range GaInAs QF lasers were reported with MOCVD growth²⁾. Although photoluminescence up to 1.224 μm was reported, 1.2 μm -range GaInAs QF lasers have not been reported with MBE growth. GaInAs QF lasers grown by MBE were only limited to around 1.12 μm , because the longer migration length in MBE-growth is apt to cause the growth of QD in a highly strained GaInAs/GaAs system. QF with a higher indium composition would be realized with good crystalline quality using a high growth rate, a low growth temperature, a high V/III pressure ratio, and a surfactant⁴⁾. With respect to surfactants, only Te has been reported so far as the surfactant for GaInAs/GaAs system. On the other hand, Sb is reported as a surfactant in Si/Ge and GaInNAs systems.

In this paper, we investigate highly strained GaInAs QF and GaInNAs QF lasers that include a small amount of Sb like a surfactant on GaAs substrates to improve the crystalline-quality by gas-source molecular-beam epitaxy (GSMBE) growth, and we studied the performance of GaInAsSb and GaInNAsSb SQW ridge lasers. In Section 2, we discuss the effects of Sb on the photoluminescence characteristics of GaInAsSb and GaInNAsSb SQW. The lasing wavelength of GaInAsSb QF lasers was increased to 1.185 μm to keep the threshold current density of as low as 280 A/cm²⁵⁾, which is one of the lowest ever reported for 1.2 μm -range GaInAs-based QF lasers. In Section 3, we fabricate ridge lasers and extract basic laser para-

* Semiconductor Research & Development Dept., Yokohama R&D Laboratories

meters such as gain coefficient, internal loss, and characteristic temperature. We report the high-performance CW lasing characteristics of 1.26 μm -GaInNAsSb SQW lasers ($I_{\text{th}}=12.4 \text{ mA}$ @25°C, $T_0=157 \text{ K}$) and 1.20 μm -GaInAsSb SQW lasers ($I_{\text{th}}=6.3 \text{ mA}$ @20°C, $T_0=256 \text{ K}$).

2. GROWTH OF SQW LASERS AND EVALUATION OF BASIC MATERIAL QUALITY

2.1 Growth Conditions of GaInNAsSb SQW

We studied GaInNAsSb SQW lasers grown by GSMBE, where the N source is a N radical generated by RF plasma cells. The lasers consisted of n-, p-GaInP cladding, a highly strained $\text{Ga}_{0.61}\text{In}_{0.39}\text{N}_{1-y}\text{As}_y\text{Sb}_{y2}$ SQW active layer (7.3 nm-thick), and 130 nm thick GaAs SCH layers located on both sides of the SQW layer. The growth temperature of the active layer and the cladding layer was set at 460°C, and the flux of AsH_3 controlled by baratron was set at 9×10^{-5} torr, and the growth rate of the well layer, which is determined by the total flux of group III, was set to 2.1 $\mu\text{m}/\text{h}$, and the flow rate of N_2 was fixed at 0.05 ccm.

To recover the crystalline quality of the GaInNAsSb layer, the lasers were annealed after growth at 650°C for 10 minutes in an atmosphere of N_2 flow. The lasers were capped by GaAs substrates to prevent the phosphorus atoms from decomposing from the surface of the epitaxial

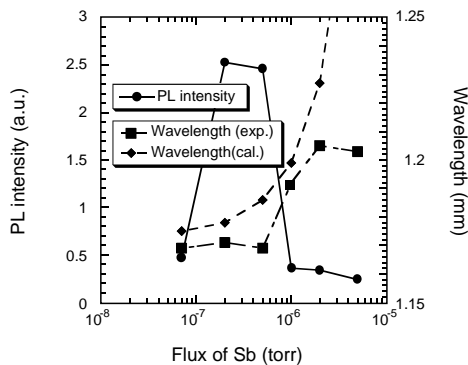


Figure 1 PL intensity and PL wavelength against Sb flux for GaInNAsSb/GaAs SQW.

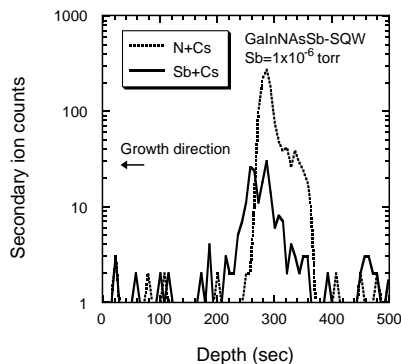


Figure 2 SIMS profile for GaInNAsSb SQW lasers with Sb flux of 1×10^{-6} torr, where N signal (Cs+N ion) and Sb signal (Cs+Sb ion) are shown.

layer. We investigated the effects of Sb on the PL characteristics. Figure 1 shows the PL intensity and the PL wavelength against the flux of Sb. With a Sb flux of 1×10^{-6} torr, where PL intensity becomes largest, the composition of SQW can be estimated as $\text{Ga}_{0.61}\text{In}_{0.39}\text{N}_{1-y-0.016}\text{As}_y\text{Sb}_{0.016}$ from the estimation of the condition of the bulk-GaAsSb layer. PL intensity of $\text{Ga}_{0.61}\text{In}_{0.39}\text{N}_{1-y-0.016}\text{As}_y\text{Sb}_{0.016}$ with Sb flux of 1×10^{-6} torr ($\lambda=1.24 \mu\text{m}$) is about one twentieth as strong as that of $\text{Ga}_{0.65}\text{In}_{0.35}\text{As}$ QF ($\lambda=1.12 \mu\text{m}$). The wavelengths of as-grown $\text{Ga}_{0.61}\text{In}_{0.39}\text{As}_{0.984}\text{Sb}_{0.016}$ and as-grown $\text{Ga}_{0.61}\text{In}_{0.39}\text{N}_{1-y-0.016}\text{As}_y\text{Sb}_{0.016}$ were 1.19 μm and 1.27 μm , respectively. We estimated N composition to be 0.44% from the wavelength shift of 80 nm. The FWHM of GaInNAsSb SQW was 23 meV, which is almost the same value as $\text{Ga}_{0.61}\text{In}_{0.39}\text{AsSb}$ SQW lasers (19 meV). Under the growth condition without Sb, FWHM becomes over 200 meV at room temperature in this composition, so we can say that Sb is very effective for suppressing 3-D growth in this material.

To investigate the crystalline-characteristics of GaInNAsSb SQW laser further, we studied the secondary ion mass spectroscopy (SIMS) and TEM for a film with various Sb contents. Figure 2 shows SIMS for GaInNAsSb SQW lasers with Sb flux of 1×10^{-6} torr, where N signal (Cs+N ion) and Sb signal (Cs+Sb ion) are shown. We calculated the integral intensity of SIMS signal from this figure, and show the relationship between the integrated intensity of Sb and N amount and the flux of Sb in Figure 3. Sb was incorporated into the GaInNAsSb-SQW layer with linearity up to the Sb flux of 2×10^{-6} torr, while the amount of N was almost constant.

Figure 4 shows TEM images for GaInNAsSb-SQW lasers with Sb flux of 2×10^{-7} torr and 1×10^{-6} torr, respectively. The SQW with Sb flux of 2×10^{-7} torr shows 3-D growth, however, the SQW with Sb flux of 1×10^{-6} torr shows 2-D growth. Sb seems to react in the GaInNAs/GaAs system like a surfactant, which restricts the formation of 3D-growth by suppressing surface diffusion caused by lowering the surface free energy.

PL intensities decrease with a Sb flux of more than 2×10^{-6} torr. The reason why the PL intensity decreases for this amount of Sb could be due to defects caused by increasing strain.

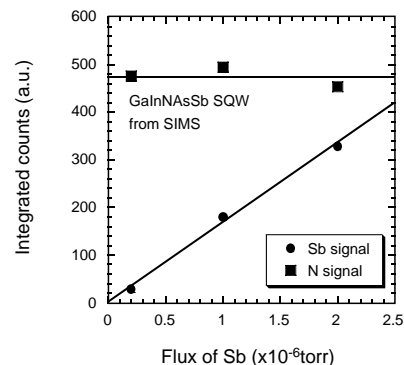


Figure 3 The integrated intensity of Sb and N in SIMS profile against the flux of Sb.

Next, we studied the effects of annealing on the PL characteristics for GaInNAsSb-SQW lasers, where N composition was decreased to 0.33% by decreasing the N radical; that is, Ga_{0.61}In_{0.39}N_{0.0033}As_{0.9807}Sb_{0.016}-SQW as shown in Figure 5. The increase of PL intensity and the blue shift caused by annealing were observed as reported in other papers. The annealing temperature of 550°C almost recovered the quality of GaInNAsSb lasers and the wavelength of the lasers annealed at 550°C was 1.23 μm and the FWHM of PL spectrum was as narrow as 23 meV.

We investigated extending the PL wavelength of GaInAs-QW film⁵⁾ using the same methods as GaInNAsSb-QW. The PL intensity becomes strongest when Sb of 2x10⁻⁷ torr is added, which is estimated as Sb composition of 0.32%. We obtained strong PL emissions up to 1.17 μm, and we confirmed that Sb also reacts like a surfactant⁵⁾.

2.2 Evaluation of Broad Contact Lasers

The threshold current density (J_{th}) and the lasing wavelength were evaluated using broad area lasers for Ga_{0.61}In_{0.39}As_{0.9968}Sb_{0.0032} and Ga_{0.61}In_{0.39}N_{0.0033}As_{0.9807}Sb_{0.016} SQW lasers. The lasing spectrum was 1.185 μm and 1.246 μm, respectively, for the lasers with a 600-μm cavity under pulse conditions shown in Figure 6 (a), (b). The lasing wavelength of GaInAsSb lasers is the longest value reported for a MBE-grown GaInAs/GaAs-QF based system to our knowledge. Figure 7 shows J_{th} against inverse cavity length. J_{th} for the lasers with 900-μm cavity was as low as 280 A/cm² for GaInAsSb lasers and 700 A/cm² for GaInNAsSb lasers, respectively, which is rela-

tively low values among the ever reported results for 1.2 μm-range GaInAs QF lasers²⁾ and 1.25~1.3 μm range GaInNAs lasers¹⁾⁻³⁾. J_{th} can be expressed as follows:

$$J_{th} = \frac{N_w J_{tr}}{\eta} \exp \left(\frac{\alpha_i + \frac{1}{2L} \ln \left(\frac{1}{R_f R_r} \right)}{N_w \xi_w G_0} \right) \quad (1)$$

where J_{tr} is the transparent current density, N_w is the number of the well, η is the spontaneous emission efficiency at the threshold, α_i is the internal loss, L is cavity length, and R_f is the reflectivity of the front facet, R_r is the reflectivity of the rear facet, ξ_w is the optical confinement factor per well, and G_0 is the gain coefficient.

The refractive index (n_r) for 1.185 μm- and 1.246 μm-light can be calculated as 3.47 and 3.46 for GaAs, and 3.18 and 3.17 for GaInP. So, the optical confinement factor can be obtained by solving Maxwell's equation as 1.99% for GaInAsSb lasers and 1.98% for GaInNAsSb lasers, respectively, assuming that n_r for GaInAsSb and GaInNAsSb is 3.52. The gain coefficient for GaInAsSb lasers and GaInNAsSb lasers assuming the logarithmic gain can be estimated as 1450 cm⁻¹ and 1700 cm⁻¹ by fitting the experimental data in Figure 7. G_0 of GaInNAsSb laser is about 1.2 times larger than that of GaInAsSb laser, which is probably due to the strong electron confinement with the deeper band offset for electrons by adding N; therefore, GaInNAsSb lasers can expect a larger T_0 compared to GaInAsSb lasers.

3. LASING CHARACTERISTICS OF RIDGE

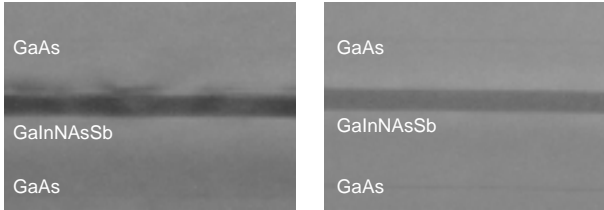


Figure 4 TEM images for GaInNAsSb-SQW lasers with Sb of 2x10⁻⁷ torr (a) and 1x10⁻⁶ torr (b), respectively.

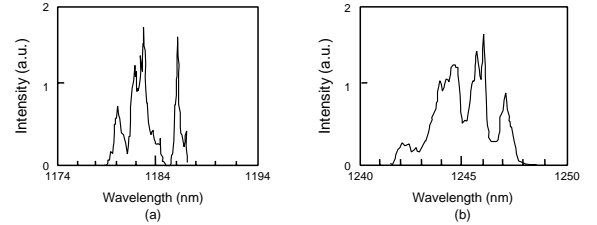


Figure 6 The lasing spectrum for broad contact lasers with a 600-μm cavity for GaInAsSb SQW laser (a), and GaInNAsSb SQW laser (b).

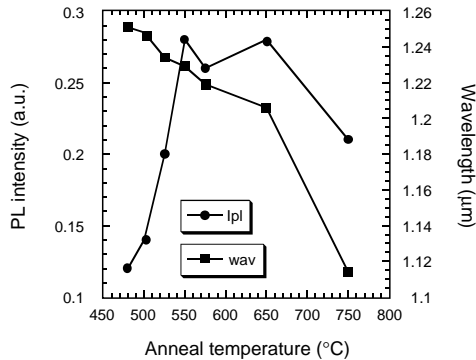


Figure 5 The effects of annealing on the PL intensities and PL wavelength for GaInNAsSb-SQW lasers, where N composition was decreased to 0.33%.

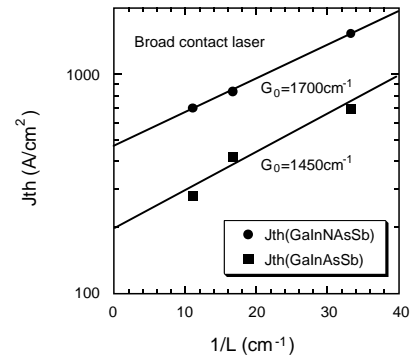


Figure 7 J_{th} against inverse cavity length for broad contact lasers of GaInAsSb and GaInNAsSb SQW lasers.

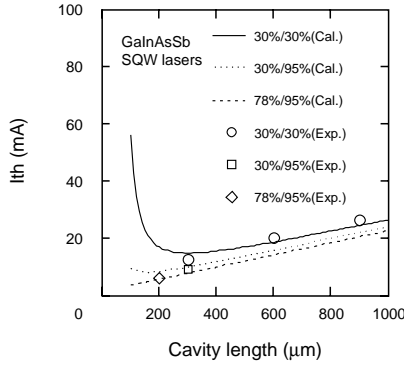


Figure 8 I_{th} against cavity length for GaInAsSb SQW lasers with a facet reflectivity parameter. The lines are theoretical curves calculated using equation (2).

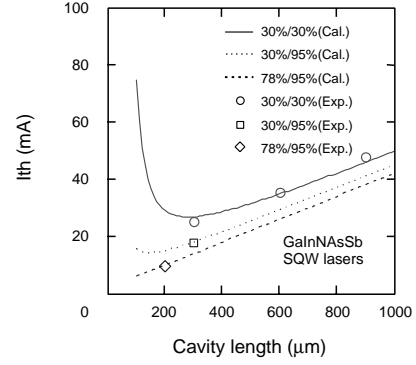


Figure 9 I_{th} against cavity length for GaInNAsSb SQW lasers with a facet reflectivity parameter. The lines are theoretical curves calculated using equation (2).

LASERS

We fabricated ridge lasers with a reverse mesa structure. The off-ridge was etched by selective wet etching to the interface between n-InGaP cladding and GaAs optical confinement layer using a SiNx mask. A solution of tartaric acid and hydrogen peroxide was used to etch the GaAs layers and hydrochloric acid was used to etch the GaInP layers. The widths at the bottom of the ridge were about 4.3 μm for both types of laser.

3.1 Evaluation of Threshold Current and Laser Parameters

Internal loss (α_i) and internal efficiency (η_i) were evaluated from cavity length dependency of external differential quantum efficiency for GaInAsSb and GaInNAsSb, and α_i and η_i were estimated as 7 cm⁻¹ and 100% for both types of laser. J_{tr}/η can be solved as 150 A/cm² for GaInAsSb lasers and 380 A/cm² for GaInNAsSb lasers, respectively, by fitting the experimental results in Figure 7, substituting α_i into equation (1). J_{tr}/η of GaInNAsSb lasers is about 2.5 times larger than that of GaInAsSb lasers, mainly because of the poor spontaneous emission efficiency (η) of GaInNAsSb lasers. The further optimization of GaInNAsSb QW growth conditions will improve the value of η , which will result in a further reduction of GaInNAsSb lasers.

The experimental I_{th} for GaInAsSb lasers and GaInNAsSb lasers are plotted in Figure 8 and Figure 9, respectively, along with the theoretical curves as a function of facet reflectivity. The threshold current (I_{th}) of the ridge lasers can be expressed as follows:

$$I_{th} = WL \frac{N_w J_{tr}}{\eta} \exp \left(\frac{\alpha_i + \frac{1}{2L} \ln \left(\frac{1}{R_l R_r} \right)}{N_w \xi_w G_0} \right) + I_1 L + I_2 \quad (2)$$

where W is the width at the bottom of the ridges, and $I_1 L + I_2$ is the leakage current, in which I_1 and I_2 are constant values. We referred the value of I_1 and I_2 reported previously in the analysis of 980 nm-InGaAs/AlGaAs SQW ridge lasers. I_2 value was set to the same value that reported in the paper ($I_2 = 0.78$ mA). I_1 was determined by

fitting the experimental threshold currents of the lasers with cleaved facets ($L = 300, 600, 900$ μm). I_1 were determined as 1.3×10^{-2} mA/μm for GaInAsSb lasers and 2×10^{-2} mA/μm for GaInNAsSb lasers. I_{th} for GaInAsSb were 12.5 mA, 20 mA, and 26 mA for cavity lengths of 300 μm, 600 μm, and 900 μm, respectively with pulse operation at 25°C. I_{th} for GaInNAsSb were 25 mA, 35 mA, and 47 mA for cavity lengths of 300 μm, 600 μm, and 900 μm, respectively with pulse operation at 25°C. The minimum I_{th} of the short cavity lasers ($L = 200$ μm) with high reflectivity (HR) coatings on both facets (SiO₂/α-Si; 78%/95%) exhibit values as low as 6 mA and 9.5 mA for GaInAsSb lasers and GaInNAsSb lasers, respectively. Here, note that I_{th} for lasers with HR coatings (CL/HR, HR/HR) agrees well with the theoretical curves.

The temperature dependence of light output power against injected current (L - I) characteristics was investigated for lasers ($L = 300$ μm, CL/95%) at pulse conditions shown in Figure 10 (a) for GaInAsSb lasers and (b) for GaInNAsSb lasers. The slope efficiencies at 25°C were 0.46 W/A for GaInAsSb and 0.44 W/A for GaInNAsSb lasers. The maximum oscillating temperatures were 145°C for GaInAsSb and 95°C for GaInNAsSb lasers. Figure 11 shows the temperature dependence of I_{th} for these lasers, where we can see that the characteristic temperatures are 120 K (@25-125°C) for GaInAsSb lasers and 111 K (@25-85°C) for GaInNAsSb lasers. Figure 12 shows the temperature dependence of the maximum slope efficiencies for these lasers. The decreasing rate of the maximum slope efficiencies were -0.010 dB/K (@25-125°C) for GaInAsSb and -0.022 dB/K (@25-75°C) for GaInNAsSb lasers. Although the band offset for the electron becomes larger by adding N into the well, the temperature dependence of L - I curves of GaInNAsSb lasers deteriorated compared to GaInAsSb lasers. This could be due to the poor crystalline of GaInNAsSb lasers; therefore, further improvement can be expected by optimizing the growth conditions of the GaInNAsSb QW layer.

3.2 DC Characteristics of Ridge Lasers

The short cavity lasers ($L = 200$ μm) with high reflection (HR) coatings on both facets ($R_l/R_r = 78\%/95\%$) were test-

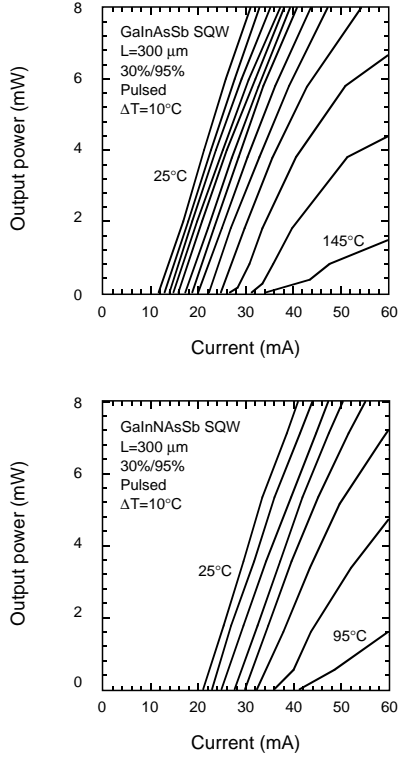


Figure 10 The temperature dependence of light-current characteristics for GaInAsSb lasers (a), and GaInNAsSb lasers (b) under pulsed operation ($L=300\ \mu\text{m}$, 30%/95%).

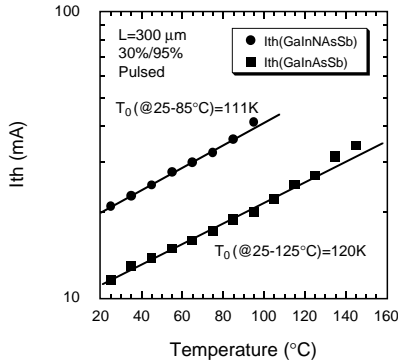


Figure 11 The temperature dependence of threshold currents for GaInAsSb and GaInNAsSb SQW lasers under pulsed operation ($L=300\ \mu\text{m}$, 30%/95%).

ed under CW operation. Figure 13 shows the temperature dependence of the light-current characteristics for GaInNAsSb lasers. The low I_{th} of 12.4 mA at 25°C was obtained under CW operation, which is almost the same value with the best results reported for narrow stripe lasers^{3), 6)}. The lasing wavelength is 1.258 μm as shown in the inset of Figure 13. A large T_0 of 157 K was obtained in the range of 25-85°C while keeping I_{th} low; therefore, this is the best result for GaInNAs-based edge emission lasers with the low I_{th} and the large T_0 to our knowledge^{3), 6)}. Further, a relatively high slope efficiency of 0.22 W/A at 25°C, a superior decreasing rate of the maximum slope efficiency of -0.014 dB/K (@25-85°C), and a CW oscillat-

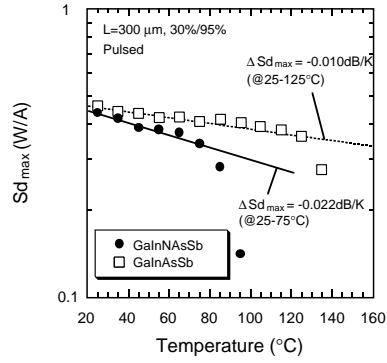


Figure 12 The temperature dependence of slope efficiency for GaInAsSb and GaInNAsSb SQW lasers under pulse operation ($L=300\ \mu\text{m}$, 30%/95%).

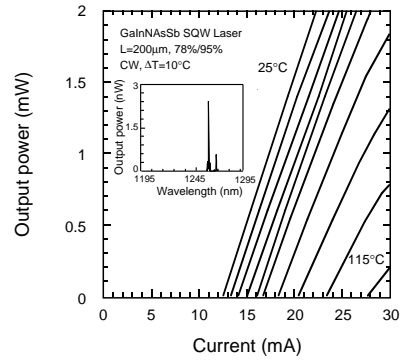


Figure 13 The temperature dependence of light-current characteristics for GaInNAsSb lasers under CW operation ($L=200\ \mu\text{m}$, 78%/95%). The inset shows lasing spectrum at room temperature.

ing at more than 100°C were obtained.

GaInAsSb lasers ($L=200\ \mu\text{m}$, 78%/95%) were also tested under CW operation. The lasing wavelength of GaInAsSb laser is 1.20 μm at 20°C, and the lasers show lower I_{th} (6.3 mA@20°C) and higher T_0 (256 K@20~70°C) compared to GaInNAsSb lasers, and it is also the best result for 1.2 μm -range highly strained GaInAs-based narrow stripe lasers⁶⁾. From these results, we can say that GaInNAsSb QF lasers are very promising for realizing peltier-free access networks and VCSELs.

4. CONCLUSIONS

Long wavelength-GaInNAsSb SQW lasers that include a small amount of Sb, were successfully grown on GaAs substrates by GSMBE. We confirmed that Sb reacts in a highly strained GaInAs/GaAs system and a GaInNAs/GaAs system like a surfactant, which increases the critical thickness at which the growth mode changes from 2-dimensional (2-D) growth to 3-dimensional (3-D) growth. Low CW I_{th} (12.4 mA) with high T_0 (157 K) and oscillation over 100°C were obtained for 1.26 μm GaInNAsSb SQW ridge lasers, and low CW I_{th} (6.3 mA) with high T_0 (256 K) was obtained for 1.20 μm GaInAsSb

SQW ridge lasers. Both types of laser produced the best results ever reported for GaInNAs-based edge emission lasers and highly strained GaInAs-based edge emission lasers with low I_{th} and high T_0 to our knowledge. GaInNAsSb QF lasers are very promising for realizing peltier-free access networks.

ACKNOWLEDGMENT

The authors would like to thank Mr. J. Kikawa for his encouragement throughout this study. Further, we also acknowledge Dr. M. Yokozeki, Dr. S. Yoshida, Dr. Y. Hiratani, and Mr. T. Kurobe for their helpful discussions on RF-GSMBE growth.

REFERENCES

- 1) M. Kondow et al., Jpn. J. Appl. Phys., vol. 35, p. 5711, 1996.
- 2) S. Sato et al., IEEE Photon. Technol. Lett., vol. 11, p. 1560, 1999.
- 3) S. Illek, Electron. Lett., vol. 36, p. 725, 2000.
- 4) M. Copel et al., Phys. Rev. Lett., vol. 63, p. 632, 1989.
- 5) H. Shimizu et al., Electron. Lett., vol. 36, p.1379, 2000.
- 6) H. Shimizu et al., Electron. Lett., vol. 36, p.1701, 2000.

Manuscript received on May 25, 2001.